The Astrophysical Journal Letters, 724:L153–L157, 2010 December 1 doi:10.1088/2041-8205/724/2/L153


# TOTAL MOLECULAR GAS MASSES OF $z \sim 3$ LYMAN- BREAK GALAXIES: CO($J = 1 \rightarrow 0$) EMISSION IN MS 1512−cB58 AND THE COSMIC EYE

Dominik A. Riechers[1,4], Christopher L. Carilli[2], Fabian Walter[3], and Emmanuel Momjian[2]
[1] Astronomy Department, California Institute of Technology, MC 249-17, 1200 East California Boulevard, Pasadena, CA 91125, USA; dr@caltech.edu
[2] National Radio Astronomy Observatory, P.O. Box O, Socorro, NM 87801, USA
[3] Max-Planck-Institut für Astronomie, Königstuhl 17, D-69117 Heidelberg, Germany
*Received 2010 August 31; accepted 2010 October 20; published 2010 November 8*

## ABSTRACT

We report the detection of CO($J = 1 \rightarrow 0$) emission toward the lensed $L^{\star}_{\rm UV}$ Lyman-break galaxies (LBGs) MS 1512−cB58 ($z = 2.73$) and the Cosmic Eye ($z = 3.07$), using the Expanded Very Large Array. The strength of the CO line emission reveals molecular gas reservoirs with masses of $(4.6 \pm 1.1) \times 10^8$ $(\mu_{\rm L}/32)^{-1}$ $(\alpha_{\rm CO}/0.8)$ $M_{\odot}$ and $(9.3 \pm 1.6) \times 10^8$ $(\mu_{\rm L}/28)^{-1}$ $(\alpha_{\rm CO}/0.8)$ $M_{\odot}$, respectively. These observations suggest ∼30%–40% larger gas reservoirs than previously estimated based on CO($J = 3 \rightarrow 2$) observations due to subthermal excitation of the $J = 3$ line. These observations also suggest gas mass fractions of $0.46 \pm 0.17$ and $0.16 \pm 0.06$. The CO($J = 1 \rightarrow 0$) emission in the Cosmic Eye is slightly resolved on scales of $4\farcs5 \pm 1\farcs5$, consistent with previous studies of nebular emission lines. This suggests that the molecular gas is associated with the most intensely star-forming regions seen in the ultraviolet (UV). We do not resolve the CO($J = 1 \rightarrow 0$) emission in cB58 at $\sim 2''$ resolution, but find that the CO($J = 1 \rightarrow 0$) emission is also consistent with the position of the UV-brightest emission peak. The gas masses, gas fractions, moderate CO line excitation, and star formation efficiencies in these galaxies are consistent with what is found in nearby luminous infrared galaxies. These observations thus currently represent the best constraints on the molecular gas content of "ordinary" (i.e., $\sim L^{\star}_{\rm UV}$) $z \sim 3$ star-forming galaxies. Despite comparable star formation rates, the gas properties of these young LBGs seem to be different from the recently identified optical/infrared-selected high-$z$ massive, gas-rich star-forming galaxies, which are more gas-rich and massive, but have lower star formation efficiencies, and presumably trace a different galaxy population.

*Key words:* cosmology: observations – galaxies: active – galaxies: formation – galaxies: high-redshift – galaxies: starburst – radio lines: galaxies

## 1. INTRODUCTION

A substantial fraction of the star formation rate density (SFRD) of the universe at $z > 2$ occurs in young star-forming galaxies that can be identified through a significant Lyman break in their spectra, so-called Lyman-break galaxies (LBGs; e.g., Steidel et al. 1996). It was recently suggested that >25% of the stellar mass in the universe was formed in LBGs (Reddy & Steidel 2009). These galaxies typically have UV-derived star formation rates (SFRs) in excess of 10 $M_{\odot}$ yr$^{-1}$ (e.g., Nandra et al. 2002; Reddy et al. 2010), marking comparatively moderate star formation events in view of the ∼2 orders of magnitude higher SFRs usually found in distant submillimeter galaxies (SMGs) and quasars (e.g., Blain et al. 2002; Wang et al. 2008). However, due to the presence of dust in the star-forming regions, their exact properties (and thus, the absolute contribution to the SFRD) are difficult to determine (e.g., Reddy et al. 2006; Wilkins et al. 2008; Carilli et al. 2008; Siana et al. 2008). It is thus desirable to study the gas and dust properties of LBGs directly, in particular through molecular line emission.

Due to the low (stellar) masses and gas content of LBGs (e.g., Shapley et al. 2003; compared to other systems observed at high redshift, e.g., SMGs and quasars), such studies are currently only possible in strongly lensed systems. Due to lensing magnification factors of ∼30, two $z \sim 3$ lensed LBGs were successfully detected in CO($J = 3 \rightarrow 2$) emission (Baker et al. 2004; Coppin et al. 2007). These observations revealed the presence of substantial amounts of molecular gas. However, recent studies of the ground-state CO($J = 1 \rightarrow 0$) transition in high-$z$ galaxies have shown that this line appears to carry a higher luminosity than higher-$J$ CO lines in many cases, and that the ratio appears to be a function of galaxy type (e.g., Riechers et al. 2006, 2010; Hainline et al. 2006; Dannerbauer et al. 2009; Ivison et al. 2010; Carilli et al. 2010; Harris et al. 2010; Aravena et al. 2010). Thus, CO($J = 1 \rightarrow 0$) observations are crucial to determine the total molecular gas content in high-$z$ galaxies, independent of gas excitation conditions. To address this issue for LBGs, we have targeted both LBGs previously detected in CO($J = 3 \rightarrow 2$) emission in the CO($J = 1 \rightarrow 0$) line.

In this Letter, we report the detection of CO($J = 1 \rightarrow 0$) emission toward the strongly lensed $L^{\star}_{\rm UV}$ $z \sim 3$ LBGs MS 1512−cB58 (Yee et al. 1996; Pettini et al. 2000, 2002) and the Cosmic Eye (Smail et al. 2007), using the Expanded Very Large Array (EVLA). We use a concordance, flat ΛCDM cosmology throughout, with $H_0 = 71$ km s$^{-1}$ Mpc$^{-1}$, $\Omega_{\rm M} = 0.27$, and $\Omega_{\Lambda} = 0.73$ (Spergel et al. 2003, 2007).

## 2. OBSERVATIONS

We observed the CO($J = 1 \rightarrow 0$) ($\nu_{\rm rest} = 115.2712$ GHz) emission line toward the Cosmic Eye and MS 1512−cB58 (hereafter: cB58) using the EVLA. At $z = 3.074$ and 2.727, this line is redshifted to 28.2944 and 30.9287 GHz (10.6 and 9.7 mm), respectively. Observations were carried out under good 9 mm weather conditions during four tracks in D array between 2009 December 4 and 28, resulting in 8.2 and 7.3 hr on-source time with 16 and 15 antennas after rejection of bad data. The nearby quasars J2134-0153 (distance to the Cosmic Eye: $0\fdg5$) and J1506+3730 (distance to cB58: $1\fdg5$) were observed every 3.5 minutes for pointing, secondary amplitude, and phase

[4] Hubble Fellow

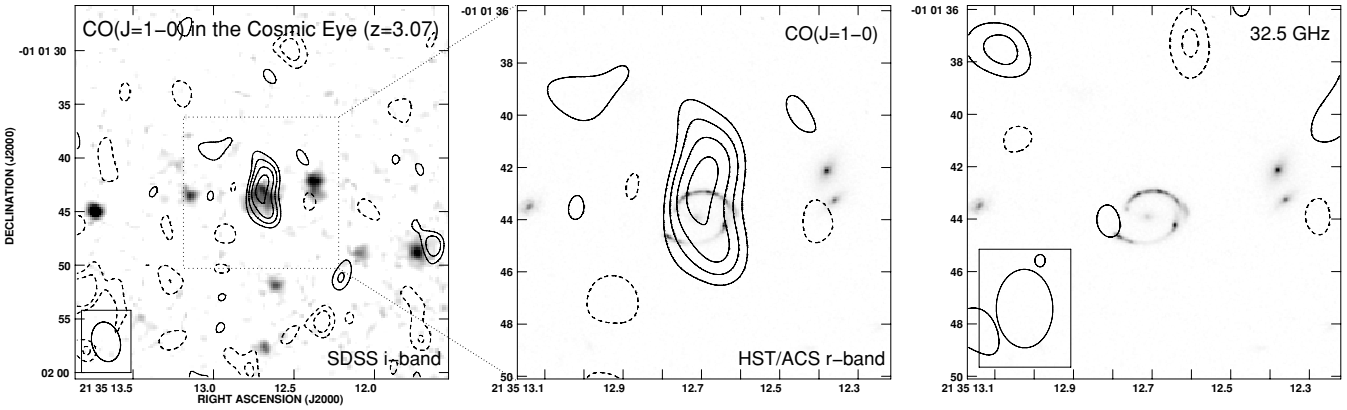


**Figure 1.** EVLA contour maps of CO($J = 1 \rightarrow 0$) emission toward the Cosmic Eye, integrated over the central 200 km s$^{-1}$ (18.75 MHz). Left: emission overlaid on a gray-scale image of the *i*-band continuum emission (from the Sloan Digital Sky Survey). Contours are shown in steps of $1\sigma = 45\,\mu$Jy beam$^{-1}$, starting at $\pm 2\sigma$. The beam size of $3\farcs4 \times 2\farcs6$ is shown in the bottom left. Middle: same contours, but zoomed-in and overlayed on a high-resolution *HST*/ACS F606W image (Smail et al. 2007). Right: same, but with 32.5 GHz contours overlaid (beam size is $3\farcs0 \times 2\farcs2$; same contour levels in all panels). No 9.2 mm continuum emission is detected down to a $2\sigma$ limit of 72 $\mu$Jy beam$^{-1}$.

calibration. For primary flux calibration, the standard calibrators 3C48 and 3C286 were observed, leading to a calibration that is accurate within $\lesssim$10%.

Observations were carried out with the previous generation correlator and set up using two intermediate frequencies (IFs) with a bandwidth of 21.875 MHz (∼220 km s$^{-1}$, dual polarization) each, and a resolution of 3.125 MHz (∼32 km s$^{-1}$). Due to tuning restrictions, we centered the first IF on the CO($J = 1 \rightarrow 0$) line, and the second IF at 32.5 GHz to measure limits on the continuum emission close to the line.

For data reduction and analysis, the AIPS package was used. All data were mapped using "natural" weighting unless mentioned otherwise. For the Cosmic Eye, the data result in a final rms of 70/45 $\mu$Jy beam$^{-1}$ per 100/200 km s$^{-1}$ (9.375/18.75 MHz) channel at a synthesized clean beam size of $3\farcs4 \times 2\farcs6$ ($3\farcs0 \times 2\farcs2$ at 32.5 GHz). For MS1512−cB58, the data result in a final rms of 70 $\mu$Jy beam$^{-1}$ per 120 km s$^{-1}$ (12.5 MHz) channel at a synthesized clean beam size of $2\farcs9 \times 2\farcs4$ ("robust 0" weighting: $2\farcs1 \times 1\farcs8$ beam; $1\farcs9 \times 1\farcs6$ at 32.5 GHz).

## 3. RESULTS

### 3.1. The Cosmic Eye

We have detected spatially resolved CO($J = 1 \rightarrow 0$) line emission toward the $z = 3.07$ Cosmic Eye at ∼6.5$\sigma$ significance (Figure 1). From two-dimensional Gaussian fitting, we measure a deconvolved source size of $4\farcs5 \pm 1\farcs5$ along the north–south axis, consistent with the UV continuum size within the errors. The source is unresolved along the east–west axis down to $\simeq 2''$. Given the relative errors, this is also consistent with the upper limit on the size of the CO($J = 3 \rightarrow 2$) emission of $\lesssim 3''$ (Coppin et al. 2007). The peak of the CO($J = 1 \rightarrow 0$) emission (peak position: $21^{\rm h}35^{\rm m}12\fs700 \pm 0\fs013$; $-01°01'42\farcs70 \pm 0\farcs47$) is consistent with the brightest emission region along the northern lens arc of this LBG at 606 nm (*HST* *r* band; rest-frame 149 nm) and 762.5 nm (SDSS *i* band; rest-frame 187 nm; see Figure 1). We thus conclude that the CO line and UV continuum emission emerge from the same star-forming regions (leading us to adopt the same lensing magnification), contrary to previous suggestions by Coppin et al. (2007) based on CO($J = 3 \rightarrow 2$) measurements (their peak position: $21^{\rm h}35^{\rm m}12\fs62$; $-01°01'43\farcs9$; see Section 3.1 in Coppin et al. 2007). No 9.2 mm continuum emission is detected down to a $2\sigma$ limit of 72 $\mu$Jy beam$^{-1}$ (Figure 1; right panel).

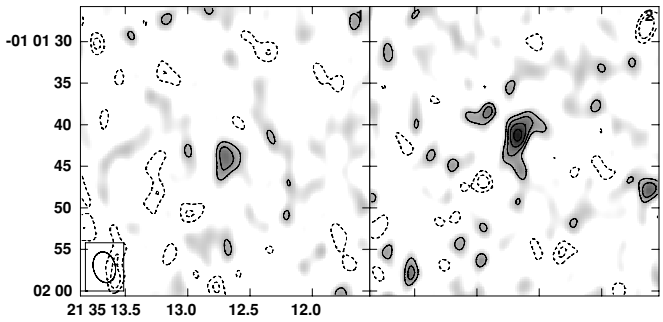

**Figure 2.** Red/blue channel maps of the CO($J = 1 \rightarrow 0$) emission in the Cosmic Eye. The same region is shown as in Figure 1 (left). One channel width is 100 km s$^{-1}$ (9.375 MHz). Contours are shown in steps of $1\sigma = 70\,\mu$Jy beam$^{-1}$, starting at $\pm 2\sigma$. The beam size is shown in the bottom left.

In Figure 2, the CO($J = 1 \rightarrow 0$) emission is shown in two 100 km s$^{-1}$ wide, red and blue velocity channels. Within the limited signal-to-noise ratio, the channel maps indicate that the emission is not only spatially, but also dynamically resolved, with molecular gas moving from north to south between the blue and red line wings. Due to the source's complex lensing morphology, the direction of the velocity gradient cannot simply be translated into a rotation axis in the source plane. Higher resolution and signal-to-noise observations with the full EVLA are required to investigate the dynamical structure of the gas reservoir in more detail.

From the Gaussian fit, we measure a line peak strength of $262 \pm 45\,\mu$Jy beam$^{-1}$, and a spatially integrated strength of $365 \pm 107\,\mu$Jy (over 200 km s$^{-1}$, comparable to the CO $J = 3 \rightarrow 2$ line FWHM of 190 km s$^{-1}$; Coppin et al. 2007). This corresponds to a CO($J = 1 \rightarrow 0$) line intensity of $I_{\rm CO} = 0.077 \pm 0.013$ Jy km s$^{-1}$, and a line luminosity of $L'_{\rm CO(1-0)} = (3.27 \pm 0.56) \times 10^{10}\ \mu_{\rm L}^{-1}$ K km s$^{-1}$ pc$^2$ (where $\mu_{\rm L}$ is the lensing magnification factor). We also derive a CO $J = 3 \rightarrow 2/1 \rightarrow 0$ line brightness temperature ratio[5] of $r_{31} = 0.72 \pm 0.16$, suggesting that the CO($J = 3 \rightarrow 2$) line is subthermally excited.

[5] We here assume that the CO($J = 1 \rightarrow 0$) and CO($J = 3 \rightarrow 2$) emission emerge from the same gas component, and thus are lensed by the same $\mu_{\rm L}$.

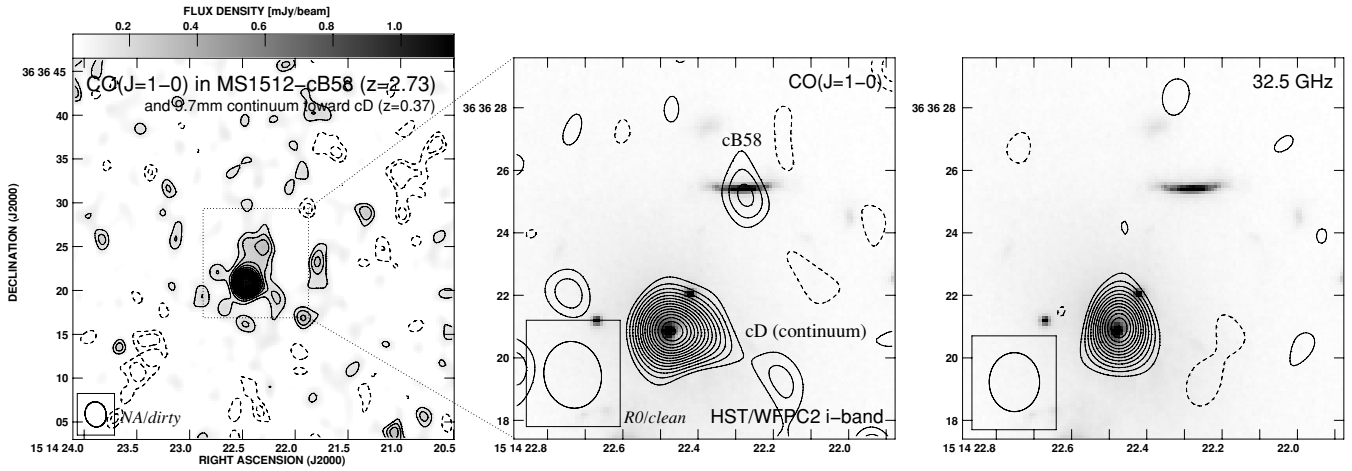


**Figure 3.** Contour maps of CO($J = 1 \rightarrow 0$) emission toward MS 1512−cB58, integrated over the central 120 km s$^{-1}$ (12.5 MHz). Left: dirty image of the emission, imaged using "natural" weighting. The second, brighter source is radio continuum emission from the cD galaxy of the foreground lensing cluster. Contours are shown in steps of $1\sigma = 70\,\mu$Jy beam$^{-1}$, starting at $\pm 2\sigma$. The beam size of $2\farcs9 \times 2\farcs4$ is shown in the bottom left. Middle: cleaned image of the same, but zoomed-in, imaged using "robust 0" weighting, and overlaid on a high-resolution *HST*/WFPC2 F814W image (image from the Hubble Legacy Archive). The beam size of $2\farcs1 \times 1\farcs8$ is shown in the bottom left. Right: same, but with 32.5 GHz contours overlaid (beam size is $1\farcs9 \times 1\farcs6$; same contour levels in all panels). No 9.2 mm continuum emission is detected toward cB58 down to a $2\sigma$ limit of 96 $\mu$Jy beam$^{-1}$.

### 3.2. MS 1512−cB58

We have detected CO($J = 1 \rightarrow 0$) emission toward the main lens arc of the $z = 2.73$ LBG MS 1512−cB58 at $\sim 4.5\sigma$ significance (Figure 3).[6] Within $\sim 4\farcs5$ of cB58, we detect a second, several times brighter source ($0.98 \pm 0.05$ and $1.21 \pm 0.07$ mJy at 9.2 and 9.7 mm), which we interpret to be continuum emission from the cD galaxy in the lensing cluster in front of cB58 at $z = 0.37$ (see gray scale 814 nm image in the middle panel of Figure 3). This separation is only $\sim 1.5 \times$ the resolution along the separation axis (imaging the data with "natural" weighting), which is sufficient for identification of both sources, but results in some flux contribution of the cD galaxy at the position of cB58 (due to sidelobe structure in the synthesized beam; see "dirty" map in the left panel of Figure 3). To properly separate the flux from both sources, we thus imaged the emission with "robust 0" baseline weighting (yielding higher spatial resolution) before applying the CLEAN algorithm (Figure 3; middle panel). Within the errors, the peak of the CO($J = 1 \rightarrow 0$) emission is consistent with the peak of the 814 nm (*HST i* band; rest-frame 218 nm) continuum emission (Figure 3; middle panel). No 9.2 mm continuum emission is detected toward cB58 down to a $2\sigma$ limit of 96 $\mu$Jy beam$^{-1}$ (Figure 3; right panel).

After deconvolution using "robust 0" weighting, we measure a CO($J = 1 \rightarrow 0$) line peak strength of $285 \pm 70\,\mu$Jy for cB58. This corresponds to $I_{\rm CO} = 0.052 \pm 0.013$ Jy km s$^{-1}$ (assuming a line FWHM of 174 km s$^{-1}$ as for the CO $J = 3 \rightarrow 2$ line; Baker et al. 2004), and $L'_{\rm CO(1-0)} = (1.82 \pm 0.45) \times 10^{10}\,\mu_{\rm L}^{-1}$ K km s$^{-1}$ pc$^2$. We find $r_{31} = 0.78 \pm 0.25$, similar to what is found for the Cosmic Eye. We also set an upper limit of $r_{71} < 0.25$ ($3\sigma$) on the CO $J = 7 \rightarrow 6/1 \rightarrow 0$ ratio.

## 4. ANALYSIS AND DISCUSSION

### 4.1. Total Molecular Gas Masses

Gas masses in LBGs are typically constrained from their H$\alpha$ luminosity, converting the (extinction-corrected) H$\alpha$ flux into an SFR, and then using the star formation law (e.g., Kennicutt 1998) to convert the SFR to molecular gas mass ($M_{\rm gas}$; e.g., Erb et al. 2006). Besides its intrinsic scatter, the star formation law implicitly depends on a conversion factor from $L'_{\rm CO}$ to $M_{\rm gas}$ ($\alpha_{\rm CO}$), yielding (at least) four considerable sources of uncertainty in such estimates.

Gas mass estimates based on CO($J = 1 \rightarrow 0$) depend on $\alpha_{\rm CO}$, but are independent of other sources of uncertainty that are inherent to alternative estimators. Thus, CO($J = 1 \rightarrow 0$) is the best known diagnostic to constrain total molecular gas masses in galaxies. Motivated by our findings below, we here adopt $\alpha_{\rm CO} = 0.8\,M_\odot$ (K km s$^{-1}$ pc$^2$)$^{-1}$, as found in nearby luminous and ultra-luminous infrared galaxies ((U)LIRGs; Downes & Solomon 1998), rather than the higher values suggested for spirals (see, e.g., Solomon & Vanden Bout 2005). Adopting $\mu_{\rm L} = 28$ (Dye et al. 2007) and $\mu_{\rm L} = 32$ (Seitz et al. 1998; Baker et al. 2004), this yields $M_{\rm gas} = (9.3 \pm 1.6) \times 10^8\,(\mu_{\rm L}/28)^{-1}\,(\alpha_{\rm CO}/0.8)\,M_\odot$ and $M_{\rm gas} = (4.6 \pm 1.1) \times 10^8\,(\mu_{\rm L}/32)^{-1}\,(\alpha_{\rm CO}/0.8)\,M_\odot$ for the Cosmic Eye and cB58, respectively.

### 4.2. Specific Star Formation Rates and Mass Doubling Timescales

Due to the presence of substantial amounts of dust and the typically young age of LBGs, estimates of SFRs and stellar masses ($M_\star$) usually agree only within a factor of a few between different estimators and fits to the spectral energy distribution (e.g., Carilli et al. 2008; Siana et al. 2008). For cB58, we adopt an SFR of $(25 \pm 10)\,M_\odot$ yr$^{-1}$ and $M_\star = (1.0 \pm 0.3) \times 10^9\,M_\odot$, as well as an infrared luminosity of $L_{\rm IR} = (1.5 \pm 0.8) \times 10^{11}\,L_\odot$ (Baker et al. 2004; Siana et al. 2008; see also Pettini et al. 2000, 2002). For the Cosmic Eye, we adopt an SFR of $140 \pm 80\,M_\odot$ yr$^{-1}$, $M_\star = (6 \pm 2) \times 10^9\,M_\odot$, and $L_{\rm IR} = (8.3 \pm 4.4) \times 10^{11}\,L_\odot$ (Coppin et al. 2007; Siana et al. 2009).

These literature values yield specific star formation rates (SSFRs; i.e., SFR/$M_\star$) of $25 \pm 12$ Gyr$^{-1}$ and $23 \pm 15$ Gyr$^{-1}$ and stellar mass doubling timescales of $\tau_{\rm double} = 40 \pm 20$ Myr and $43 \pm 28$ Myr for cB58 and the Cosmic Eye, respectively. Despite the fact that both sources are $\sim L^\star_{\rm UV}$ LBGs at $z \sim 3$, their SSFRs are $\sim 5 \times$ higher and their $\tau_{\rm double}$ are $\sim 5 \times$ lower than the median values for $z \sim 3$ LBGs (4.3 Gyr$^{-1}$ and 230 Myr; e.g.,

[6] We do not detect the $>10 \times$ less magnified counter image (Seitz et al. 1998), as expected.

Magdis et al. 2010). We estimate that both the SSFR and $\tau_{\rm double}$ in cB58 and the Cosmic Eye are by a factor of ∼3 uncertain (in particular due to the difficulty in constraining any old part of their stellar populations; Siana et al. 2008), and thus, may well fall within the scatter of the values found for the general (unlensed) LBG population. If taken at face value, this could also imply that cB58 and the Cosmic Eye are close to the peak intensity of the starbursts that drive the buildup of their stellar mass, when their SSFRs may reach levels comparable to those in $z > 2$ SMGs (15–30 Gyr$^{-1}$; e.g., Daddi et al. 2009; Tacconi et al. 2008). Indeed, both cB58 and the Cosmic Eye appear to be comparatively young LBGs (<300 Myr; e.g., Siana et al. 2008, 2009).

### 4.3. Gas Fractions, Depletion Timescales, and Star Formation Efficiencies

Both of our targets are gas rich. We find gas mass fractions[7,8] of $f_{\rm gas}^{0.8} = M_{\rm gas}/M_\star = 0.46 \pm 0.17$ and $0.16 \pm 0.06$ and baryonic gas mass fractions of $f_{\rm bary}^{\rm g,0.8} = M_{\rm gas}/(M_{\rm gas}{+}M_\star) = 0.32 \pm 0.08$ and $0.13 \pm 0.04$ for cB58 and the Cosmic Eye, respectively. These values are comparable to nearby luminous and ultra-luminous infrared galaxies, but (on average) somewhat lower than in SMGs (typical $f_{\rm bary}^{\rm g}$∼0.4; Tacconi et al. 2006, 2008) and high-$z$ massive, gas-rich star-forming galaxies (hereafter SFGs;[9] typical $f_{\rm bary}^{\rm g}$∼0.45–0.6; e.g., Daddi et al. 2008, 2010a; Tacconi et al. 2010). The comparatively high $f_{\rm gas}$ and $f_{\rm bary}^{\rm g}$ in cB58 are also consistent with its relatively young age (<30 Myr; Siana et al. 2008), and thus, a relatively early phase in its starburst. On the other hand, cB58 may have had a higher SFR in the past if all of its estimated stellar mass were build up in the ongoing starburst within <30 Myr.

The minimum times for which the starbursts can be maintained at their current rates are given by the gas depletion timescales, which we find to be $\tau_{\rm dep}^{0.8} = M_{\rm gas}/{\rm SFR} \sim 18 \pm 8$ Myr and $\sim 7 \pm 4$ Myr for cB58 and the Cosmic Eye, respectively.[10] These are by a factor of a few shorter than in SMGs (<100 Myr; e.g., Greve et al. 2005) and >30 × shorter than in SFGs (∼0.5–0.9 Gyr; e.g., Daddi et al. 2008; Tacconi et al. 2010). However, SMGs have typically 10–50 × higher SFRs than these LBGs, while SFGs have comparable SFRs.

The ratio between $L_{\rm IR}$ ($\propto$SFR) and $L'_{\rm CO}$ ($\propto M_{\rm gas}$) can be used as a measure of the star formation efficiency. We find ratios of $\sim 260 \pm 150$ and $\sim 710 \pm 390$ for cB58 and the Cosmic Eye, respectively, comparable to what is found in nearby ULIRGs and SMGs (typically ∼250, but with large scatter up to >1000; e.g., Tacconi et al. 2006, 2008), and substantially higher than the ratios found in nearby spiral galaxies (typically ∼30–60; e.g., Gao & Solomon 2004). However, SMGs have ∼40 × higher median $L'_{\rm CO}$ and $M_{\rm gas}$, and ∼3 × broader CO lines than these LBGs (e.g., Coppin et al. 2008).[11]

[7] An index 0.8 indicates that $\alpha_{\rm CO} = 0.8\ M_\odot\ ({\rm K\ km\ s^{-1}\ pc^2})^{-1}$ is assumed.

[8] We do not derive $M_{\rm dyn}$-based gas fractions due to the limited constraints on the CO sizes and dynamics.

[9] These are galaxies with SFRs of $>50\ M_\odot\ {\rm yr}^{-1}$ and $M_\star > 3 \times 10^{10}\ M_\odot$ selected in the UV/optical/near-infrared; referred to in the literature as, e.g., "BzK" galaxies, "BX/BM"/AEGIS galaxies, or "normal" high-$z$ star-forming galaxies (e.g., Daddi et al. 2010a; Tacconi et al. 2010).

[10] The main differences relative to previous values are the different adopted $\alpha_{\rm CO}$ and a small overcorrection for the excitation of the CO($J = 3 \rightarrow 2$) line in cB58 (Baker et al. 2004), and the different adopted $\mu_{\rm L}$(CO) and SFR for the Cosmic Eye (Coppin et al. 2007).

[11] Some SFGs have similarly narrow CO lines, but likely just due to low disk inclinations (e.g., Daddi et al. 2010a).

### 4.4. Sizes of the Gas Reservoirs

Detailed studies of nebular emission lines in the rest-frame UV/optical suggest that cB58 and the Cosmic Eye have intrinsic sizes of ∼1–2 kpc (e.g., Seitz et al. 1998; Stark et al. 2008), indicating that they are more compact than SMGs and SFGs (e.g., Tacconi et al. 2008, 2010; Carilli et al. 2010; Daddi et al. 2010a). The extent of the CO($J = 1 \rightarrow 0$) emission in these $z \sim 3$ $L^\star_{\rm UV}$ LBGs is consistent with that of the UV/optical light. It thus is unlikely that the gas is distributed on scales as large as typical for the above types of galaxies.

## 5. CONCLUSIONS

We have detected luminous CO($J = 1 \rightarrow 0$) emission toward the gravitationally lensed $\sim L^\star_{\rm UV}(z \simeq 3)$ LBGs cB58 ($z = 2.73$) and the Cosmic Eye ($z = 3.07$). The ground-state CO line carries 30%–40% more luminosity than the previously detected CO($J = 3 \rightarrow 2$) lines in these galaxies. This implies that the $J = 3$ lines are subthermally excited. The gas masses, gas excitation, gas fractions, and star formation efficiencies in these $z \sim 3$ LBGs are consistent with nearby luminous infrared galaxies, which also matches their observed $L_{\rm IR}$. These LBGs have comparable SFRs to SFGs (Daddi et al. 2008, 2010a; Tacconi et al. 2010), but their gas properties suggest that their star formation mode is consistent with starbursts, rather than these high-$z$ disk galaxies (which harbor comparatively long-lasting star formation at low efficiencies; see Daddi et al. 2010b; Genzel et al. 2010). Even though the star formation *mode* and SSFRs are consistent with SMGs at similar $z$, these LBGs are substantially less massive, less extreme, less extended, and (likely) less dust-obscured systems. While SMGs may trace a brief, but common phase in the evolution of massive galaxies, LBGs thus probably trace a common phase in the formation of more "typical" (i.e., $\sim L^\star$) present-day galaxies (e.g., Somerville et al. 2001; Adelberger et al. 2005; Conroy et al. 2008).

This consistent picture is obtained if one chooses a ULIRG-like $\alpha_{\rm CO}$ conversion factor, and helps to motivate it. Both cB58 and the Cosmic Eye are thought to have slightly sub-solar metallicities ($z \simeq 0.4$ and $0.9\ Z_\odot$; e.g., Baker et al. 2004; Stark et al. 2008), which may require some modification to $\alpha_{\rm CO}$. However, as already discussed by Baker et al. (2004), there is no consensus in the literature on how severe the impact of metallicity on $\alpha_{\rm CO}$ really is, in particular due to the fact that the CO lines arise in optically thick gas. We thus do not modify $\alpha_{\rm CO}$ from the canonical value for ULIRGs found by Downes & Solomon (1998), but do acknowledge the typical factor of a few uncertainty inherent to this assumption (see also discussion by Coppin et al. 2007).

The observations presented here revise the masses and some of the physical properties of the gas reservoirs in the lensed $z \sim 3$ LBGs cB58 and the Cosmic Eye, highlighting the importance of CO($J = 1 \rightarrow 0$) observations in comparatively "ordinary" (i.e., $\sim L^\star_{\rm UV}$) high-$z$ galaxies. The gas reservoirs in both systems are consistent with those in starburst regions of nearby luminous infrared galaxies, providing supporting evidence that LBGs mark intense star formation events in common, relatively low-mass galaxies at high $z$ (in comparison to SMGs). The conditions for star formation appear markedly different from those in the massive, gas-rich star-forming galaxies at high $z$ that were discovered recently (SFGs; Daddi et al. 2008, 2010a; Tacconi et al. 2010), which are typically more gas rich and massive, but have lower star formation efficiencies.

The present investigation thus has identified differences between the gas properties of differently selected, comparatively common high-$z$ star-forming galaxies that host less extreme star formation events than SMGs and far-infrared-luminous high-$z$ quasars. With the rising capabilities of the EVLA to study high-$z$ CO($J = 1 \rightarrow 0$) emission in a more unbiased manner, we thus are beginning to unravel the different contributors to the gas mass and star formation histories of the universe in a more direct way than possible so far.

We thank the referee for a helpful report. D.R. acknowledges support from from NASA through Hubble Fellowship grant HST-HF-51235.01 awarded by STScI, operated by AURA for NASA, under contract NAS 5-26555. NRAO is a facility of NSF operated under a cooperative agreement by AUI.

## REFERENCES

Adelberger, K. L., et al. 2005, ApJ, 619, 697
Aravena, M., et al. 2010, ApJ, 718, 177
Baker, A. J., et al. 2004, ApJ, 604, 125
Blain, A. W., et al. 2002, Phys. Rep., 369, 111
Carilli, C. L., et al. 2008, ApJ, 689, 883
Carilli, C. L., et al. 2010, ApJ, 714, 1407
Conroy, C., et al. 2008, ApJ, 679, 1192
Coppin, K., et al. 2007, ApJ, 665, 936
Coppin, K., et al. 2008, MNRAS, 389, 45
Daddi, E., et al. 2008, ApJ, 673, L21
Daddi, E., et al. 2009, ApJ, 694, 1517
Daddi, E., et al. 2010a, ApJ, 713, 686
Daddi, E., et al. 2010b, ApJ, 714, L118
Dannerbauer, H., et al. 2009, ApJ, 698, L178
Downes, D., & Solomon, P. M. 1998, ApJ, 507, 615
Dye, S., et al. 2007, MNRAS, 379, 308
Erb, D. K., et al. 2006, ApJ, 646, 107
Gao, Y., & Solomon, P. M. 2004, ApJ, 606, 271
Genzel, R., et al. 2010, MNRAS, 407, 2091
Greve, T. R., et al. 2005, MNRAS, 359, 1165
Hainline, L. J., et al. 2006, ApJ, 650, 614
Harris, A. I., et al. 2010, ApJ, 723, 1139
Ivison, R. J., et al. 2010, MNRAS, 404, 198
Kennicutt, R. C. 1998, ApJ, 498, 541
Magdis, G. E., et al. 2010, ApJ, 720, L185
Nandra, K., et al. 2002, ApJ, 576, 625
Pettini, M., et al. 2000, ApJ, 528, 96
Pettini, M., et al. 2002, ApJ, 569, 742
Reddy, N. S., & Steidel, C. C. 2009, ApJ, 692, 778
Reddy, N. S., et al. 2006, ApJ, 644, 792
Reddy, N. S., et al. 2010, ApJ, 712, 1070
Riechers, D. A., et al. 2006, ApJ, 650, 604
Riechers, D. A., et al. 2010, ApJ, 720, L131
Seitz, S., et al. 1998, MNRAS, 298, 945
Shapley, A. E., et al. 2003, ApJ, 588, 65
Siana, B., et al. 2008, ApJ, 689, 59
Siana, B., et al. 2009, ApJ, 698, 1273
Smail, I., et al. 2007, ApJ, 654, L33
Solomon, P. M., & Vanden Bout, P. A. 2005, ARA&A, 43, 677
Somerville, R. S., Primack, J. R., & Faber, S. M. 2001, MNRAS, 320, 504
Spergel, D. N., Bean, R., & Doré, O., et al. 2007, ApJS, 170, 377
Spergel, D. N., Verde, L., & Peiris, H. V., et al. 2003, ApJS, 148, 175
Stark, D. P., et al. 2008, Nature, 455, 775
Steidel, C. C., et al. 1996, ApJ, 462, L17
Tacconi, L. J., et al. 2006, ApJ, 640, 228
Tacconi, L. J., et al. 2008, ApJ, 680, 246
Tacconi, L. J., et al. 2010, Nature, 463, 781
Wang, R., et al. 2008, ApJ, 687, 848
Wilkins, S. M., et al. 2008, MNRAS, 385, 687
Yee, H. K. C., et al. 1996, AJ, 111, 1783